*Journal of Biomaterials and Tissue Engineering*
Vol. 4, 1–7, 2014

# A Three-Dimensional Finite Element Study to Characterize the Influence of Load Direction on Stress Distribution in Bone Around Dental Implant

Darush Zia Shamami[1,2], Alireza Karimi[1,2], Borhan Beigzadeh[2,*], Shahram Derakhshan[2], and Mahdi Navidbakhsh[1,2]

[1] *Tissue Engineering and Biological Systems Research Laboratory, School of Mechanical Engineering, Iran University of Science and Technology, Tehran 16846, Iran*
[2] *School of Mechanical Engineering, Iran University of Science and Technology, Tehran 16846, Iran*

This study aimed to establish a three-dimensional (3D) finite element model for variation of loading direction to identify its effects on the stress distribution generated around an implant and surrounding jawbone under biomechanical consideration. Twenty one 3D finite element cases containing the endosseous titanium implant in type II bone under three different loads i.e., 50, 100, and 200 N, with various directions from 0 to 30 degrees to the vertical axis with the increasing rate of 5 degrees were applied to analyze the stress distribution pattern in the implant and surrounding bone. For data analysis, the von Mises criterion was used. The results revealed that the oblique loading would significantly induce higher interfacial stresses compared to the vertical loading. The highest on Mises stress was observed in the implant for all the cases. An increasement of the angle of force both increased the maximum stress and worsened stress distribution patterns in the implant and supporting bone. The results suggest that under oblique load 30° the maximum von Mises stresses in the implant, cortical, and cancellous bones increase by 236%, 322%, and 22%, respectively. The findings of this study may have implications not only for understanding the stress distribution in implant and bone under various loading angles but also for determining an optimum implant for specific application in dentistry.

**Keywords:** Dental Implant, Finite Element Analysis, Stress Analysis, Jawbone, Load Direction.

RESEARCH ARTICLE

## 1. INTRODUCTION

Endosseous dental implants play pivotal role in prosthodontics and restorative dentistry since the early 1970s.[1] Owing to its reliable functional and aesthetic results, dental rehabilitation with implants has been widely accepted by doctors and patients in recent decades.[2] High implant success rates of the order of 78–100% have been reported, with more than 25 years of observation time.[3–5] Despite these high success rates, implant failure, marginal bone loss, and patient discomfort still sometimes occur.[6–8] Generally speaking, the success of dental implants is correlated to the biologic tissues (soft tissue and bone) response and mechanical components strength (implant components and superstructures) as well as surgical technique.[9,10] One of the reasons for implant failure is Occlusal overload or fatigue-induced microdamage.[11] Implants may also fail due to the loss of bone surrounding the implant.[12] Bone loss usually begins at the crestal area of the cortical bone and can progress toward the apical region, jeopardizing the longevity of the implant and prosthesis.[13] Stress and strain fields around osseointegrated dental implants are affected by a number of biomechanical factors, including the type of loading, material properties of the implant and the prosthesis, implant geometry, surface structure, quality and quantity of the surrounding bone as well as the nature of the bone-implant interface.[14,15] Biomechanical factors are important for longevity of osseointegrated implants. Controlling these factors prevents mechanical complications, which include fracture of screws, components, or materials veneering the framework.[16] The application of engineering knowledge in dentistry has contributed to an understanding of biomechanical aspects related to implantology.[17] Finite element analysis (FEA) was initially developed in the early 1960s to solve structural problems in the aerospace industry but has since been extended to implant dentistry.[18] The bone stress distribution pattern is highly relevant to the bone-implant relationship and consequently to its

*Author to whom correspondence should be addressed.


2157-9083/2014/4/001/007
doi:10.1166/jbt.2014.1230

longevity.[19] There are some studies which investigated the influence of occlusal overloading[13, 20] and oblique forces[16, 21–23] on the bone around dental implants. It has been indicated that overloading and load angles should be considered as the very important factors in loss of osseointegration of dental implants. However, a few studies focused on the load direction and its effects on the stress distribution pattern around dental implants. The purpose of this study is to evaluate the effects of external loading under various directions on the stress distribution in the dental implant and surrounding jawbone using 3D finite element analysis.

## 2. MATERIALS AND METHODS

The 3D finite element models were built with CATIA V5R19 software and ABAQUS 6.10-1 software (SIMULIA Corporation, providence, RI, United States) to analyze the stress distributions. The model contained abutment, implant, cortical, and cancellous bones, which three values for load assigned to it, including 50, 100, and 200 N. The model was subjected to loading at various directions from 0 to 30 degrees to the vertical axis of implant with increasing rate of 5 degrees were applied to the system to analyze the stress distribution in the implant and supporting bone. The implant with standard diameter was presented in form of screw and abutment of conical form and adjusted to the implant. The bone was modeled as full structure that is composed of a spongy center surrounded by 2 mm of cortical bone.

### 2.1. Implant System

A Branemark implant (length and diameter of 13 and 3.9 mm, respectively) and triangular thread type (pitch = 1.25 mm) was connected to conic standard abutment (length = 5 mm, large diameter = 3.9 mm, and small diameter = 3 mm).

### 2.2. Material Properties

The materials used in the current study were assumed to be homogenous, isotropic, and linearly elastic. The physical properties of different components modeled are listed in Table I. The implant and abutment were all designed to be titanium alloy, with an elastic modulus of 110 GPa. Two types of bone density were modeled by varying the elastic modulus of compact bone and cancellous bone with elastic moduli of 13.7 and 1.37 GPa, respectively.

**Table I.** Physical properties of the different components used in this study.

| Component | Elastic modulus (GPa) | Poisson‘s ratio | Reference |
|---|---|---|---|
| Cortical bone | 13.7 | 0.3 | [59] |
| Dense cancellous bone | 1.37 | 0.3 | [59] |
| Titanium | 110 | 0.33 | [60] |

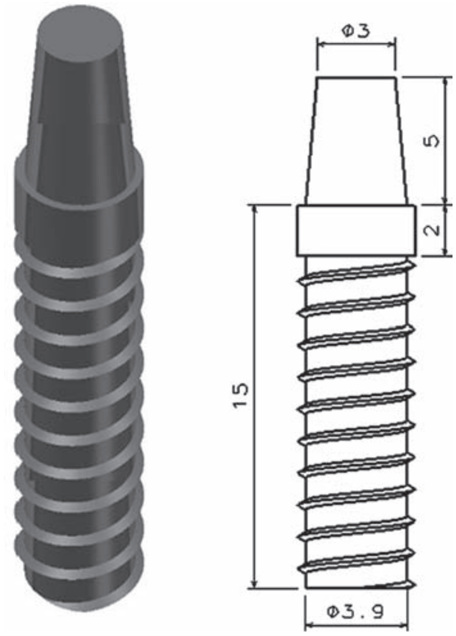


**Fig. 1.** The model design of specimen components and interface condition of the implant.

### 2.3. Model Design and Interface Conditions

Three values of load, i.e., 50, 100, and 200 N, were applied to each set of the model, such as the abutment and implant, with various directions of load from 0 to 30 degrees to the vertical axis of implant with the increasing rate of 5 degrees. Abutment height of the models was modified to 5 mm from the crown margin to the top of the abutment. Implant was connected to conic standard abutment. The rough surface of the testing fixture with 13 mm length was totally embedded in the bone, and interface conditions between the bone and implant were assumed to be fully osseointegrated. The crown margin to the crestal bone level was designed with the same distance of 2 mm (Fig. 1).

### 2.4. Model Building and Geometry

The bone model was simplified to a cuboid form (14 mm × 14 mm × 25 mm) and was classified as type II bone; type II bone consisted of a layer of cortical bone with uniform thickness of 2 mm, which was surrounded by a core of dense cancellous bone. The 3D model was built by CATIA computer aided design program, which is capable of input geometric features such as length, angle, diameter, and profile to make drawings of the sample parts and assemblies (Fig. 2).

### 2.5. Elements and Nodes

Finite element model was executed with one implant system, which contained one type of fixture in combination with one type of bone quality; the numbers of elements and nodes were well refined in the model.



RESEARCH ARTICLE

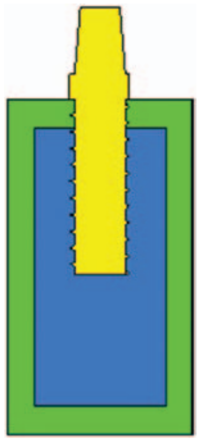

**Fig. 2.** Plane diagram illustrating the model design and geometry of the implant with the rough surface totally embedded in bone. Key: yellow = implant and abutment; green = cortical bone; blue = cancellous bone.

The refined mesh of the abutment and implant were all set to an element size of 0.5 mm, whereas the crestal cortical and cancellous bones were all set to an element size of 1.3 mm.

### 2.6. Finite Element Analyses

The finite element analyses were performed to calculate the von Mises stress distribution.[24] Computer-aided engineering software was used to input a 3D model of the sample and defined the mesh control of the model. After meshing the 3D model, conditions such as loads, constraints, and materials were assigned. Three values of load (50, 100, and 200 N) under various directions were applied in order to analyze the stress distribution in the implant and supporting bone. The loads were applied separately on the center point of the abutment (Fig. 3).

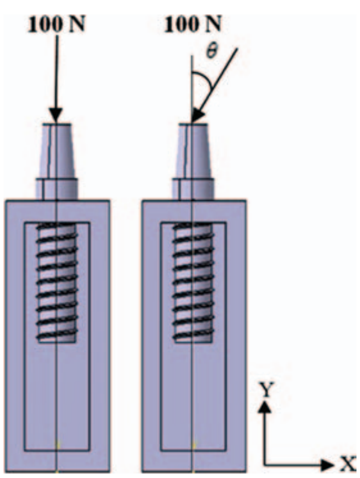


**Fig. 3.** The loads were applied under different directions from 0 to 30 degrees to the vertical axis of implant with the increasing rate of 5 degree in XY plane.

**Table II.** Maximum von Mises stress (Mpa) in different components of model under A 50-N force with various loading angles.

| Loading angle (degree) | 0 | 5 | 10 | 15 | 20 | 25 | 30 |
|---|---|---|---|---|---|---|---|
| Implant | 14.43 | 20.44 | 26.45 | 32.34 | 38.02 | 43.44 | 48.53 |
| Cortical bone | 2.04 | 3.31 | 4.45 | 5.56 | 6.63 | 7.65 | 8.61 |
| Cancellous bone | 0.457 | 0.462 | 0.464 | 0.463 | 0.466 | 0.515 | 0.559 |

## 3. RESULTS

The stress field in each case with different loading angles was investigated carefully. The maximum von Mises stresses obtained in the implant and surrounding jawbone with applied load directions from 0 to 30 degrees are shown in Tables II, III, and IV for 50, 100, 200 N force, respectively. The highest maximum von Mises stress was observed in the implant for all the cases. It can be seen that stress concentrations occurred at the thread tips of the implant in the neck region near the cortical bone. In the surrounding jawbone, the maximum effective stress under all loading directions occurred at the regions adjacent to the first thread of implant. The maximum effective stress induced by the oblique load was much higher than that of the maximum effective stress caused by an equal amount of vertical load. Furthermore, an increase in the angle of force application caused not only an increasement of maximum stress values but also worsened the stress distribution patterns in the implant and supporting bone. In the other words, the angle of force application had a significant effect on both the contour patterns and the magnitude of stress fields. Under an axial loading condition, the stress fields showed a symmetric pattern, whereas they exhibited an asymmetric pattern in the case of oblique loading (Figs. 4–6). The results showed that under oblique load (30°) the maximum von Mises stresses in the implant, cortical, and cancellous bones increase by 236%, 322% and 22%, respectively. Moreover, the maximum stresses in the implant and surrounding jawbone as a function of loading angle are shown in Figure 7 for all simulated cases. It is clear that the maximum stress in the cancellous bone remained almost constant with increasing angles of force application, exhibiting insensitivity to loading direction. However, the maximum stress in the implant and cortical bone significantly changed with varied loading angles.

**Table III.** Maximum von Mises stress (Mpa) in different components of model under A 100-N force with various loading angles.

| Loading angle (degree) | 0 | 5 | 10 | 15 | 20 | 25 | 30 |
|---|---|---|---|---|---|---|---|
| Implant | 28.85 | 40.89 | 52.91 | 64.69 | 76.05 | 86.87 | 97.08 |
| Cortical bone | 4.08 | 6.63 | 8.90 | 11.12 | 13.26 | 15.30 | 17.22 |
| Cancellous bone | 0.914 | 0.923 | 0.927 | 0.926 | 0.932 | 1.029 | 1.119 |

**Table IV.** Maximum von Mises stress (Mpa) in different components of model under A 200-N force with various loading angles.

| Loading angle (degree) | 0 | 5 | 10 | 15 | 20 | 25 | 30 |
|---|---|---|---|---|---|---|---|
| Implant | 57.71 | 81.76 | 105.83 | 129.38 | 152.09 | 173.74 | 194.14 |
| Cortical bone | 8.17 | 13.25 | 17.81 | 22.24 | 26.52 | 30.59 | 34.45 |
| Cancellous bone | 1.829 | 1.846 | 1.854 | 1.853 | 1.863 | 2.058 | 2.238 |

They increased almost linearly with an increase in the loading angle up to 30 degrees.

## 4. DISCUSSIONS

Due to the complex geometry of bone and dental implant system the closed form solutions in stress analysis is not feasible. The finite element method has been increasingly used in this field to analyze the stress distribution patterns in the implant-bone interface for different root-form implant designs.[18, 25, 26] Overloading and disadvantageous stress distribution pattern in jawbone and implant can cause resorption of the bone and failure of the implant.[11, 12] Therefore, investigation of stress field in implant/jawbone systems is of vital importance. In the present work, an implant/jawbone system in twenty one cases was numerically studied, and the effects of load direction on stress values and distribution patterns in the implant and supporting bone were investigated. Figures 4–6 display several typical contour patterns of von Mises stress and local stress distributions in regions in which the highest stress occurred in the implant and supporting bone under 100 N force and angles of 0, 15, and 30 degrees, respectively. All the results demonstrated that a higher loading angle will result in an increasing the magnitude and worsens the distribution pattern of stress. As reported in the literature,[21, 27] an increased angle of force application increases the stress concentrations in the neck region and thus increases the maximum stress values in the jawbone. Similar results

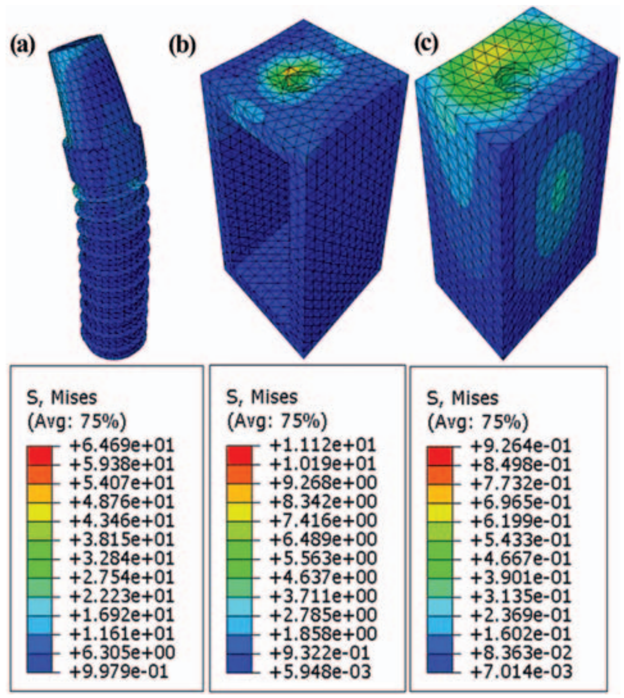


**Fig. 5.** Von Mises stress contour patterns in the (a) implant, (b) cortical bone, and (c) cancellous bone under 100 N force and angle of 15 degrees.

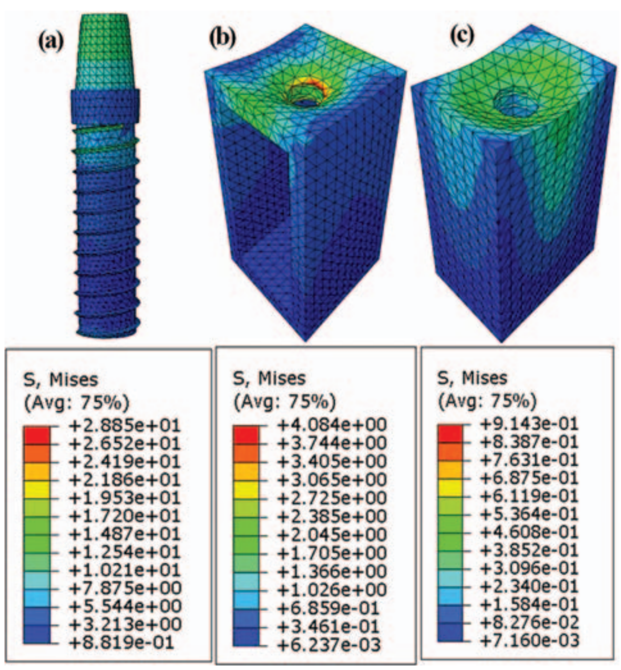


**Fig. 4.** Von Mises stress contour patterns in the (a) implant, (b) cortical bone, and (c) cancellous bone under 100 N force and angle of 0 degrees.

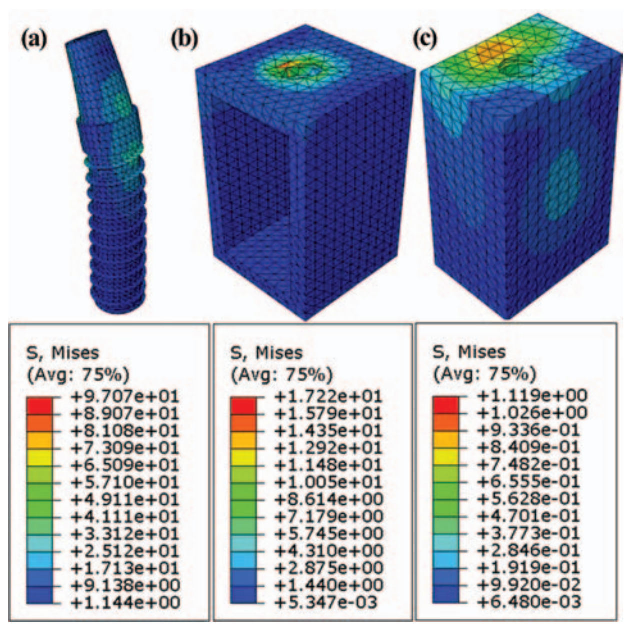


**Fig. 6.** Von Mises stress contour patterns in the (a) implant, (b) cortical bone, and (c) cancellous bone under 100 N force and angle of 30 degrees.

were obtained in the cortical and cancellous bones in the present work. Moreover, it was seen that an increased loading angle significantly worsened the stress distribution patterns. Figure 7 shows maximum von Mises stresses in different components of model as a function of loading angle for three forces. It was demonstrated that the maximum values of stress in the implant and cortical bone increased almost linearly up to loading angle of 30 degrees. However, the values of maximum stress in cancellous bone remained nearly unchanged up to 30 degrees.

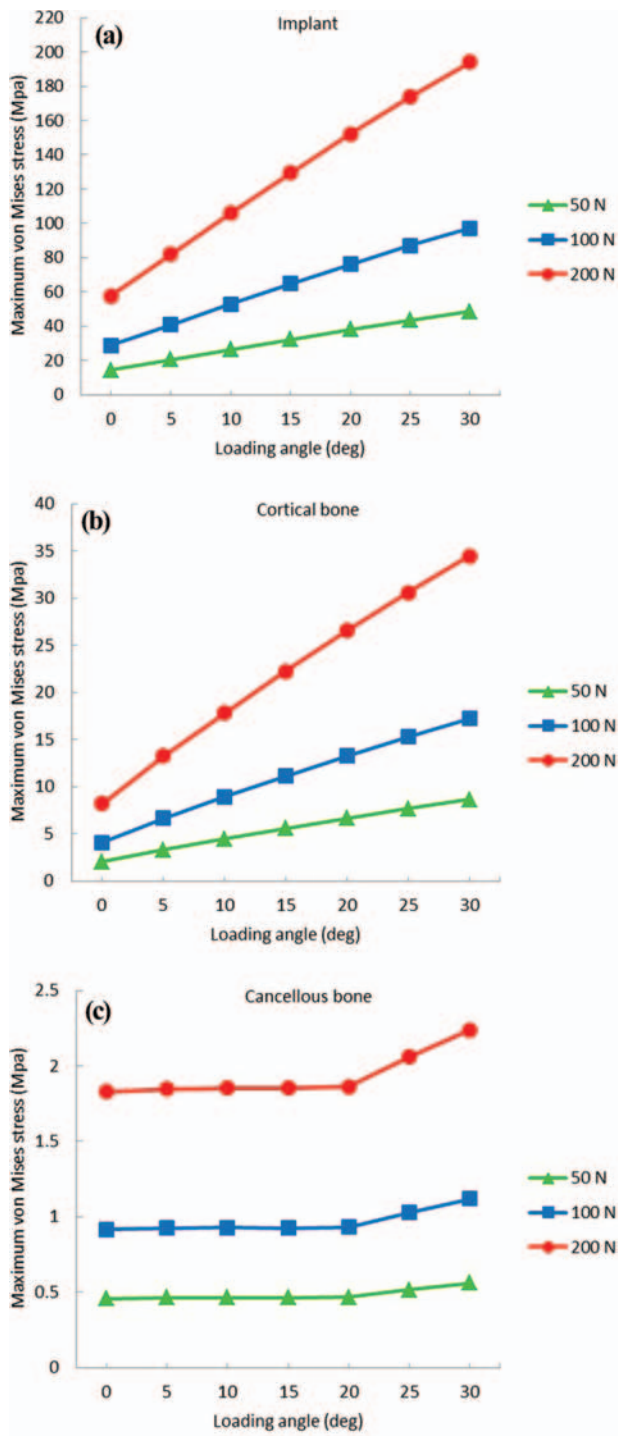


**Fig. 7.** Maximum von Mises stresses in the (a) implant, (b) cortical bone, (c) cancellous bone as a function of loading angle for different forces.

Although interesting results have found, there are still some shortcomings in this study which need to be considered. All materials in this study considered to be homogenous and isotropic.[28–33] Nonetheless, dental material may present hyperelastic[34–38] or viscoelastic[39–44] mechanical behavior rather than simple elastic one.[45–47] Therefore, there is a need to conduct an experimental study using uniaxial or biaxial tensile test machine[48–52] to measure their anisotropic visco-hyperelastic behavior.[53–58]

In general, an oblique loading angle is the most severe loading condition that significantly increases the stress values and worsens the distribution patterns. Therefore, it is highly recommended to be avoided as much as possible.

## 5. CONCLUSION

Based on the results from numerical analyses, the loading direction had a significant effect on the maximum stress values and stress distribution patterns in the implant/bone system. Increases in the angle of force application not only can increase the maximum stress values but can worsen the stress distribution patterns in the implant and supporting bone. The maximum stress in the implant and cortical bone changed greatly with varied loading angles. They increased almost linearly with an increase in the loading angle up to 30 degrees. Whereas, the maximum stress in the cancellous bone remained almost unchanged with increasing angles of force application, exhibiting insensitivity to loading direction.

### Conflicts of Interest

The authors declare that they have no conflicts of interest.

**Acknowledgments:** The authors acknowledge the Iran University of Science and Technology for funding this project.

## References and Notes

1. J. Porter and J. Von Fraunhofer, Success or failure of dental implants? A literature review with treatment considerations. *Gen. Dent.* 53, 423 (**2004**).
2. T. Li, L. Kong, Y. Wang, et al., Selection of optimal dental implant diameter and length in type IV bone: A three-dimensional finite element analysis. *Int J. Oral Maxillofac. Surg.* 38, 1077 (**2009**).
3. T. Albrektsson, E. Dahl, L. Enbom, et al., Osseointegrated oral implants: A Swedish multicenter study of 8139 consecutively inserted Nobelpharma implants. *J. Periodontol* 59, 287 (**1988**).
4. B. Engquist, T. Bergendal, T. Kallus, and U. Linden, A retrospective multicenter evaluation of osseointegrated implants supporting overdentures. *Int J. Oral Maxillofac Implants* 3, 129 (**1988**).
5. T. Jemt, U. Lekholm, and R. Adell, Osseointegrated implants in the treatment of partially edentulous patients: A preliminary study on 876 consecutively placed fixtures. *Int J. Oral Maxillofac Implants* 4, 211 (**1988**).

**6.** W. Becker and B. E. Becker, Replacement of maxillary and mandibular molars with single endosseous implant restorations: A retrospective study. *J. Prosthet Dent.* 74, 51 (**1995**).

**7.** M. Expósito, J. Hirsch, U. Lekholm, and P. Thomsen, Biological factors contributing to failures of osseointegrated oral implants.(I). Success criteria and epidemiology. *Eur J. Oral Sci.* 106, 527 (**2008**).

**8.** C. J. Goodacre, J. Y. Kan, and K. Rungcharassaeng, Clinical complications of osseointegrated implants. *J. Prosthet Dent.* 81, 537 (**1999**).

**9.** L. Vidyasagar and P. Apse, Biological response to dental implant loading/overloading. Implant overloading: empiricism or science. *Stomatologija* 5, 83 (**2003**).

**10.** O. Dilek, E. Tezulas, and M. Dincel, Required minimum primary stability and torque values for immediate loading of mini dental implants: An experimental study in nonviable bovine femoral bone. *Oral Surg. Oral Med. Oral Pathol Oral Radiol Endod.* 105, 20 (**2008**).

**11.** M. Esposito, P. Thomsen, L. E. Ericson, L. Sennerby, and U. Lekholm, Histopathologic observations on late oral implant failures. *Clin. Implant Dent. Relat. Res.* 2, 18 (**2000**).

**12.** L. Qian, M. Todo, Y. Matsushita, and K. Koyano, Effects of implant diameter, insertion depth, and loading angle on stress/strain fields in implant/jawbone systems: finite element analysis. *Int J. Oral Maxillofac Implants* 24, 877 (**2008**).

**13.** F. Isidor, Loss of osseointegration caused by occlusal load of oral implants. A clinical and radiographic study in monkeys. *Clin. Oral Implants Res.* 7, 143 (**1996**).

**14.** G. Watzek, Endosseous Implants: Scientific and Clinical Aspects: Quintessence Pub Co (**1996**).

**15.** M. S. Block, J. N. Kent, and L. Guerra, Implants in dentistry: essentials of endosseous implants for maxillofacial reconstruction: Saunders (**1997**).

**16.** J. F. Santiago Junior, E. P. Pellizzer, F. R. Verri, and P. S. P. de Carvalho, Stress analysis in bone tissue around single implants with different diameters and veneering materials: A 3-D finite element study. *Mater. Sci. Eng. C* 33, 4700 (**2013**).

**17.** S. Sahin and M. C. Çehreli, The significance of passive framework fit in implant prosthodontics: Current status. *Implant Dent.* 10, 85 (**2001**).

**18.** J. P. Geng, K. B. Tan, and G. R. Liu, Application of finite element analysis in implant dentistry: A review of the literature. *J. Prosthet Dent.* 85, 585 (**2001**).

**19.** M. Cruz, T. Wassall, E. M. Toledo, L. Barra, and A. Lemonge, Three-dimensional finite element stress analysis of a cuneiform-geometry implant. *Int J. Oral Maxillofac Implants* 18, 675 (**2002**).

**20.** T. Miyata, Y. Kobayashi, H. Araki, T. Ohto, and K. Shin, The influence of controlled occlusal overload on peri-implant tissue. Part 3: A histologic study in monkeys. *Int J. Oral Maxillofac Implants* 15, 425 (**1999**).

**21.** H. J. Chun, S. Y. Cheong, J. H. Han, et al., Evaluation of design parameters of osseointegrated dental implants using finite element analysis. *J. Oral Rehabil* 29, 565 (**2002**).

**22.** H. S. Chang, Y. C. Chen, Y. D. Hsieh, and M. L. Hsu, Stress distribution of two commercial dental implant systems: A three-dimensional finite element analysis. *J. Dent. Sci.* 8, 261 (**2013**).

**23.** N. Djebbar, B. Serier, B. B. Bouiadjra, S. Benbarek, and A. Drai, Analysis of the effect of load direction on the stress distribution in dental implant. *Mater. Des.* 31, 2097 (**2010**).

**24.** M. Shahmohammadi, H. Asgharzadeh Shirazi, A. Karimi, and M. Navidbakhsh, Finite element simulation of an artificial intervertebral disk using fiber reinforced laminated composite model. *Tissue Cell* (**2014**); In press. DOI: http://dx.doi.org/10.1016/j.tice.2014.05.008.

**25.** S. Hansson, The implant neck: Smooth or provided with retention elements. A biomechanical approach. *Clin. Oral Implants Res.* 10, 394 (**1999**).

**26.** D. Siegele and U. Soltesz, Numerical investigations of the influence of implant shape on stress distribution in the jaw bone. *Int. J. Oral Maxillofac Implants* 4, 333 (**1988**).

**27.** F. Watanabe, Y. Hata, S. Komatsu, T. C. Ramos, and H. Fukuda, Finite element analysis of the influence of implant inclination, loading position, and load direction on stress distribution. *Odontology* 91, 31 (**2003**).

**28.** A. Karimi and M. Navidbakhsh, Response to the Letter to the Editor: Measurement of the uniaxial mechanical properties of healthy and atherosclerotic human coronary arteries. *Mater. Sci. Eng. C* 42, 421 (**2014**).

**29.** A. Karimi, M. Navidbakhsh, and R. Razaghi, Dynamic simulation and finite element analysis of the human mandible injury protected by polyvinyl alcohol sponge. *Mater. Sci. Eng. C* 42, 608 (**2014**).

**30.** A. Karimi, M. Navidbakhsh, T. Rezaee, and K. Hassani, Measurement of the circumferential mechanical properties of the umbilical vein: Experimental and numerical analyses. *Comput. Methods Biomech. Biomed. Engin.* (**2014**); In press. DOI: 10.1080/10255842.2014.910513.

**31.** A. Karimi, M. Navidbakhsh, H. Yamada, and R. Razaghi, A nonlinear finite element simulation of balloon expandable stent for assessment of plaque vulnerability inside a stenotic artery. *Med. Biol. Eng. Comput.* 52, 589 (**2014**).

**32.** A. Karimi, M. Navidbakhsh, and A. Motevalli Haghi, An experimental study on the structural and mechanical properties of polyvinyl alcohol sponge using different stress–strain definitions. *Adv. Polym. Tech.* (**2014**). In press. DOI: 10.1002/adv.21441.

**33.** A. Karimi and M. Navidbakhsh, Material properties in unconfined compression of gelatin hydrogel for skin tissue engineering applications. *Biomed. Tech. (Berl)* (**2014**). In press. DOI: 10.1515/bmt-2014-0028.

**34.** A. Karimi A, M. Navidbakhsh, and R. Razaghi, Dynamic finite element simulation of the human head damage mechanics protected by polyvinyl alcohol sponge. *Int J. Damage Mech.* (**2014**); In press. DOI: 10.1177/1056789514535945.

**35.** A. Karimi, M. Navidbakhsh, B. Beigzadeh, and S. Faghihi, Hyperelastic mechanical behavior of rat brain infected by Plasmodium berghei ANKA-Experimental testing and constitutive modeling. *Int J. Damage Mech.* (**2013**); In press. DOI: 10.1177/1056789513514072.

**36.** A. Karimi, M. Navidbakhsh, and S. Faghihi. Fabrication and mechanical characterization of polyvinyl alcohol sponge for tissue engineering applications. *Perfusion* 29, 232 (**2014**).

**37.** A. Karimi, M. Navidbakhsh, H. Yousefi, A. Motevalli Haghi, and S. J. Adnani Sadati, Experimental and numerical study on the mechanical behavior of rat brain tissue. *Perfusion* (**2014**); In press. DOI: 10.1177/0267659114522088.

**38.** A. Karimi, M. Navidbakhsh, S. Faghihi, A. Shojaei, and K. Hassani, A finite element investigation on plaque vulnerability in realistic healthy and atherosclerotic human coronary arteries. *ProcI. Mecht. H* 227, 148 (**2013**).

**39.** A. Karimi and M. Navidbakhsh. Mechanical properties of PVA material for tissue engineering applications. *Mater. Tech. Adv. Perform Mater.* 29, 90 (**2014**).

**40.** A. Karimi, M. Navidbakhsh, H. Yamada, T. Rezaee, and K. Hassani, A comparative study on the quasilinear viscoelastic mechanical properties of umbilical artery and umbilical vein. *Perfusion* (**2014**); In press. DOI: 10.1177/0267659114536761.

**41.** A. Karimi, M. Navidbakhsh, and B. Beigzadeh, A visco-hyperelastic constitutive approach for modeling polyvinyl alcohol sponge. *Tissue Cell* 46, 97 (**2014**).

**42.** S. Faghihi, M. Gheysour, A. Karimi, and R. Salarian, Fabrication and mechanical characterization of graphene oxide-reinforced poly(acrylic acid)/gelatin composite hydrogels. *J. Appl. Phys.* 115, 083513 (**2014**).

**43.** A. Karimi, M. Navidbakhsh, R. Razaghi, and M. Haghpanahi, A computational fluid-structure interaction model for plaque vulnerability assessment in atherosclerotic human coronary arteries. *J. Appl. Phys.* 115, 144702 **(2014)**.

**44.** S. Faghihi, A. Karimi, M. Jamadi, R. Imani, and R. Salarian, Graphene oxide/poly(acrylic acid)/gelatin nanocomposite hydrogel: Experimental and numerical validation of hyperelastic model. *Mater. Sci. Eng. C* 38, 299 **(2014)**.

**45.** A. Karimi and M. Navidbakhsh, An experimental study on the mechanical properties of rat brain tissue using different stress–strain definitions. *J. Mater. Sci.—Mater. Med.* 25, 1623 **(2014)**.

**46.** A. Karimi, M. Navidbakhsh, H. Yousefi, and M. Alizadeh, An experimental study on the elastic modulus of gelatin hydrogel using different stress–strain definitions. *J. Thermoplast Compos Mater.* **(2014)**; In press. DOI: 10.1177/0892705714533377.

**47.** A. Karimi, M. Navidbakhsh, A. Shojaei, and S. Faghihi, Measurement of the uniaxial mechanical properties of healthy and atherosclerotic human coronary arteries. *Mater. Sci. Eng. C* 33, 2550 **(2013)**.

**48.** A. Karimi, M. Navidbakhsh, M. Alizadeh, and A. Shojaei, A comparative study on the mechanical properties of the umbilical vein and umbilical artery under uniaxial loading. *Artery Res.* 8, 51 **(2014)**.

**49.** A. Karimi, M. Navidbakhsh, A. Shojaei, K. Hassani, and S. Faghihi, Study of plaque vulnerability in coronary artery using Mooney-Rivlin model: A combination of finite element and experimental method. *Biomed. Eng. Appl. Basis Commun.* 26, 145 **(2014)**.

**50.** A. Karimi, M. Navidbakhsh, M. Alizadeh, and R. Razaghi, A comparative study on the elastic modulus of polyvinyl alcohol sponge using different stress–strain definitions. *Biomed. Tech. (Berl)* **(2014)**; In press. DOI: 10.1515/bmt-2013-0110.

**51.** A. Karimi and M. Navidbakhsh, Measurement of the nonlinear mechanical properties of PVA sponge under longitudinal and circumferential loading. *J. Appl. Polym. Sci.* 131, 40257 **(2014)**.

**52.** A. Karimi, M. Navidbakhsh, and S. Faghihi, Measurement of the mechanical failure of PVA sponge using biaxial puncture test. *J. Biomater Tissue Eng.* 4, 46 **(2014)**.

**53.** A. Karimi, M. Navidbakhsh, and M. Haghpanahi, Constitutive model for numerical analysis of polyvinyl alcohol sponge under different strain rates. *J. Thermoplast Composite Mater.* **(2014)**; In press. DOI: 10.1177/0892705713520176.

**54.** A. Karimi and M. Navidbakhsh, Mechanical properties of polyvinyl alcohol sponge under different strain rates. *Int J. Mater. Res.* 105, 404 **(2014)**.

**55.** A. Karimi, R. Faturechi, M. Navidbakhsh, and A. Hashemi, A nonlinear hyperelastic behavior to identify the mechanical properties of rat skin under uniaxial loading. *J. Mech. Med. Biol.* 14, 1450075 **(2014)**.

**56.** E. Barati, M. Halabian, A. Karimi, and M. Navidbakhsh, Numerical evaluation of stenosis location effects on hemodynamics and shear stress through curved artery. *J. Biomater Tissue Eng.* 4, 358 **(2014)**.

**57.** A. Karimi, M. Navidbakhsh, and R. Razaghi, An experimental-finite element analysis on the kinetic energy absorption capacity of polyvinyl alcohol sponge. *Mater. Sci. Eng. C* 39, 253 **(2014)**.

**58.** A. Karimi, M. Navidbakhsh, and S. Faghihi, A comparative study on plaque vulnerability using constitutive equations. *Perfusion* 29, 179 **(2014)**.

**59.** R. M. Cibirka, M. E. Razzoog, B. R. Lang, and C. S. Stohler, Determining the force absorption quotient for restorative materials used in implant occlusal surfaces. *J. Prosthet Dent.* 67, 361 **(1992)**.

**60.** E. J. Richter, B. Orschall, and S. Jovanovic, Dental implant abutment resembling the two-phase tooth mobility. *J. Biomech.* 23, 297 **(1990)**.


Received: xx xxxx xxxx. Accepted: xx xxxx xxxx.